Magnetic, electrical, structural, and thermal properties of amorphous MnSi

J. J. Hauser, F. S. L. Hsu, G. W. Kammlott, and J. V. Waszczak
Bell Laboratories, Murray Hill, New Jersey 07974
(Received 9 March 1979)

MnSi films deposited by getter sputtering at substrate temperatures lower than 650 K are amorphous as determined by x-ray diffraction, scanning-electron-microscopy, electrical-resistivity, and magnetic-susceptibility measurements. Amorphous films display a negative temperature coefficient of resistivity (TCR), while crystalline films are characterized by a positive TCR with a resistive anomaly in the vicinity of the ferromagnetic Curie temperature (T_C = 30 K). The magnetic-susceptibility measurements clearly establish that while crystalline MnSi is a ferromagnet with a T_C of 30 K, amorphous MnSi is a concentrated spin-glass with a spin-glass transition at $T_{SG} = 22 \pm 2$ K. The spin-glass transition was studied by both ac and dc susceptibility and by specific-heat measurements. The presence of amorphous ferromagnetic clusters is clearly shown by a susceptibility anomaly around 30 K, by the dependence of the susceptibility and its peak on the temperature of deposition of the films, and by the temperature dependence of the magnetic susceptibility. The independence of T_{SG} and of the spin-glass order parameter measured below T_{SG} on the degree of clustering suggests that the clusters are mediated by the same exchange interaction which governs individual spins.

I. INTRODUCTION

The word spin-glass is usually applied to dilute solid solutions such as Cu-Mn, Au-Mn, and Au-Fe which are characterized by a sharp cusplike peak in the magnetic susceptibility.[1-3] The spin-glass behavior has also been observed in concentrated alloys such as Cu-Mn,[4,5] and in such amorphous concentrated systems as $GdAl_2$,[6,7] and MnSi.[8] On the other hand, it has been shown that the susceptibility and the cusp are strongly dependent on the temperature of deposition and annealing for Cu-Mn films[9] and on such metallurgical treatment as quenching, aging, and cold working for bulk Cu-Mn alloys.[4,10,11] More recently,[12] it was shown that annealing an amorphous Au-Si-Mn spin-glass without causing recrystallization led to impressive changes in the susceptibility cusp. A similar effect was observed in the strong dependence of the susceptibility cusp of amorphous MnSi (a-MnSi) films on their deposition temperature.[8] All these studies[4,8-12] suggest that the smallest cusp corresponds to the most random distribution of Mn atoms and that the magnitude of the cusp depends on the degree of clustering of the Mn atoms. The fact that the magnitude of the cusp depends strongly on deposition temperature and annealing even in the amorphous state[8,12] suggests that the atomic redistribution leading to the amorphous clusters takes place on a very fine microscopic scale. Because a-MnSi is a concentrated spin-glass system and because of the low ferromagnetic Curie temperature (T_C) of the crystalline material, it was possible to separate the spin-glass transition and the clustering behavior.[8] The purpose of this paper is threefold: First, to present additional data from ac susceptibility, x-ray-diffraction, scanning-electron-microscopy (SEM), and electrical-resistivity experiments which were not shown in the previous brief publication[8]; second, to extend the data with dc-susceptibility and specific-heat measurements; third, to investigate the effect of nonstoichiometry on the spin-glass behavior, i.e., on both the spin-glass transition temperature (T_{SG}) and the magnitude of the susceptibility cusp.

II. EXPERIMENTAL PROCEDURE

The films deposited onto sapphire substrates at temperatures of 370 K and above were getter sputtered at 6 W (1500 V, 4 mA) with an argon pressure of about 5×10^{-2} Torr. Lower deposition temperatures (T_D) were obtained by lowering the sputtering power, e.g., 3 W (1500 V, 2 mA) for T_D = 320 K. Deposition temperatures above 370 K were achieved by resistively heating the sapphire substrate on a tantalum heater table. Films deposited at 77 K were getter sputtered at 2.25 W (1500 V, 1.5 mA) with an argon pressure of about 3×10^{-2} Torr. The sputtering targets were prepared in two different ways. The stoichiometric MnSi target was obtained by melting inductively[13] in an alumina crucible under an argon atmosphere the required amount of high-purity Mn and Si. The off-stoichiometric targets were produced by melting in an arc furnace followed by fast cooling.[13] The film thickness was determined from the weight gain using the crystalline density of 5.9 g cm^{-3} for MnSi and linear average of the densities of the constituent elements for the off-stoichiometric compositions. The amorphous nature of the films was ascertained by x-ray diffraction and SEM.

TABLE I. Properties of the MnSi x-ray and SEM samples.

Sample No.	Thickness (μm)	T_D (K)	Structure
25	11.4	370	amorphous
22	5.9	625	amorphous
20	4.8	650	13-vol. % crystalline (Fig. 5)
15	5.2	650	25-vol. % crystalline (Fig. 5)
23	4.4	675	microcrystalline
12	4.6	900	crystalline
4	1.8	370+ anneal at 900 K	crystalline

The ac susceptibility of the films was measured usually at 10 kHz with a modulating field of 4 Oe with a push rod susceptibility holder[14] by warming up the sample in helium gas from 4.2 K to room temperature. For dc susceptibility and specific-heat measurements, a large amount of material (0.16 g) was sputtered onto large sapphire wafers and scraped with a sapphire wafer. For the dc susceptibility measurement, the resulting flakes were placed in an ultra pure quartz container and measured using the Faraday method[15] by cooling the sample in zero magnetic field and applying the measuring dc field at the desired temperature. For specific-heat measurements the flakes were mounted with Apiezon grease.

The resistivity of the samples was obtained on a holder using four spring loaded contacts.

The annealing of all films was performed by heating resistivity *in vacuo* the samples on a tantalum heater table for 30 min.

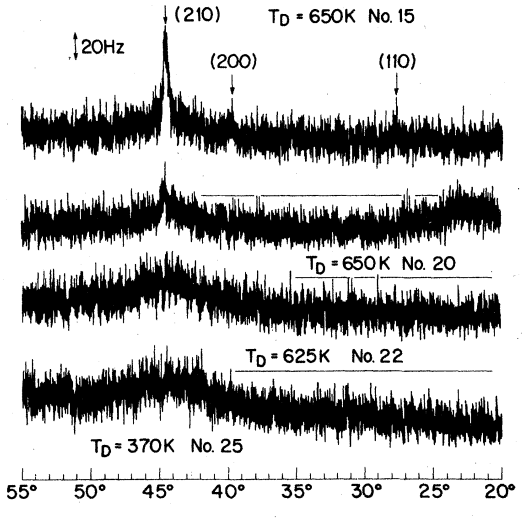

FIG. 1. X-ray diffractometer traces for amorphous and partially crystalline MnSi films. Crystalline lines are indicated by arrows.

III. EXPERIMENTAL RESULTS AND DISCUSSION

A. Structure

The properties of the films used in the structural analysis (x-ray diffraction and SEM) are listed in Table I. It is clear from Fig. 1 that films deposited below 650 K (up to 625 K) are fully amorphous. The first signs of crystallinity appear in films sputtered at 650 K. One also notices a pronounced (210) preferred orientation in all films deposited at and above 650 K (Figs. 1 and 2). A film deposited just above the threshold temperature for crystallinity (650 K) at 675 K is not yet fully crystalline as shown by the more numerous and more intense lines observed in a film deposited at 900 K (Fig. 2). The (210) preferred orientation present in as-deposited crystalline films is also present in crystalline films obtained by recrystallization of an amorphous film (Fig. 3). The amorphous state of the films can also be evidenced visually. Indeed, while amorphous films have a silver shine, crystalline films deposited above 650 K have a matty brown appearance which results from $\simeq 1$-μm platelets with a (210) preferred orientation growing perpendicularly to the plane of the film (Fig. 4).

The onset of crystallinity at 650 K revealed by the x-ray diffractometer traces of Fig. 1 is verified by the SEM shown in Fig. 5 where one can ob-

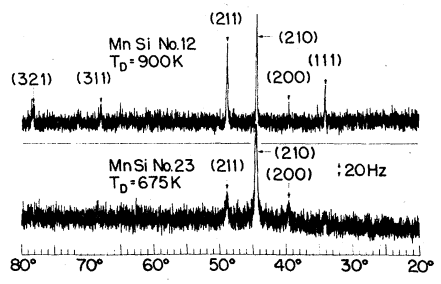

FIG. 2. X-ray diffractometer traces for MnSi films deposited in the crystalline state.

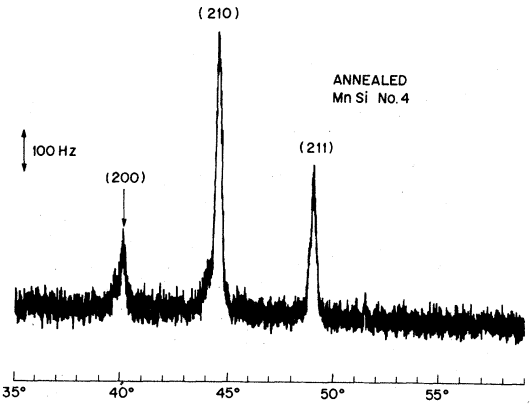

FIG. 3. X-ray diffractometer trace for an MnSi film deposited at 370 K in the amorphous state and recrystallized by annealing 15 min at 900 K in *vacuo*.

serve isolated 1-μm microcrystals embedded in an amorphous matrix. It is also noteworthy to point out that the relative x-ray line intensities for the two films MnSi No. 15 and No. 20 are in good agreement with the relative concentration of

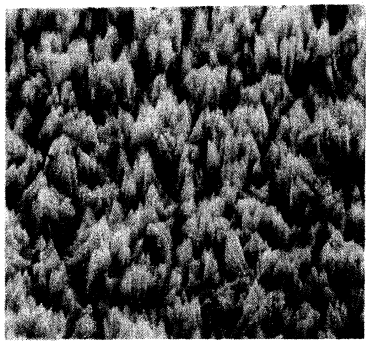

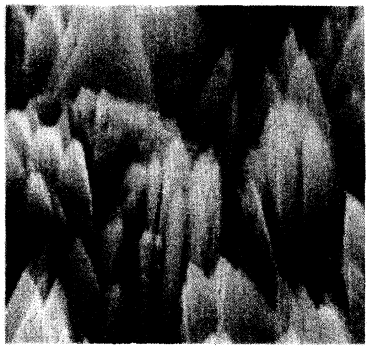

FIG. 4. Scanning electron microscopy for crystalline MnSi No. 12 deposited at 900 K (optical magnifications at 5000 $\bar{x}$ for the top picture and 20 000 $\bar{x}$ for the bottom).

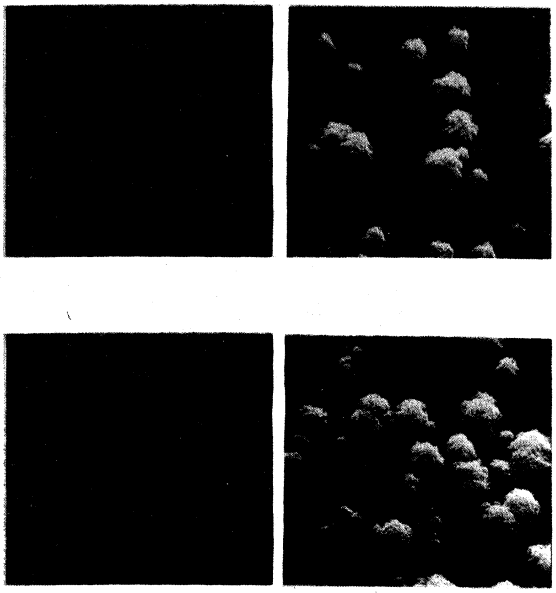

FIG. 5. Scanning electron microscopy for partially crystalline films deposted at 650 K: Top taken on MnSi No. 20 and bottom on MnSi No. 15 (the optical magnification are 1600× for the pictures on the left and 8000× for those on the right-hand side).

microcrystals seen in the SEM (Table I). This structural result of microcrystals embedded in an amorphous matrix for films deposited at 650 K is in excellent agreement with the electrical and magnetic properties of such films which will be discussed in the following sections.

The conclusion of this structural analysis is that the boundary between amorphous and crystalline films is extremely sharp ($T_D = 650$ K). Consequently, the increasing susceptibility cusp with increasing deposition temperature observed in *a*-MnSi films deposited below 650 K (Fig. 3 and Table I of Ref. 8) could not possibly be caused by microcrystalline effects, but must result from some form of clustering occurring in the amorphous state.

B. Electrical resistivity

The properties of the various amorphous and crystalline MnSi films and of the off-stoichiometric amorphous Mn-Si films used in the electrical resistivity measurements are summarized in Table II. The major result of the electrical measurements is that amorphous films can be distinguished from crystalline films by the temperature dependence of their resistivity. While *a*-MnSi films have a negative temperature coefficient of resistivity (TCR) as shown in Figs. 6 and 7 and Table II, crystalline films have a positive TCR[16] (Fig.

TABLE II. Properties of the Mn-Si resistivity samples.

Sample No.	Thickness (μm)	T_D (K)	$10^4\rho$(RT) (Ω cm)	ρ(RT)/ρ(4.2 K)	A	B	C
MnSi No. 5	0.8	370	14.9	0.82	0.84	0.17	0.020
MnSi No. 5		anneal at 1300 K	3	9.1	...	...	...
MnSi No. 6	0.9	370	9.2	0.82	0.84	0.17	0.020
MnSi No. 8	0.6	370	8.6	0.86	0.84	0.17	0.020
MnSi No. 13	4.3	500	13.9	0.82	0.89	0.12	0.029
MnSi No. 14	5.9	600	7.1	0.79	0.89	0.12	0.029
MnSi No. 15	5.2	650	19.5	0.62	...	...	...
MnSi No. 20	4.8	650	17.5	0.59	...	...	...
MnSi No. 17	5.7	700	5.6	2.2	...	...	...
MnSi No. 16	5.0	800	6.6	2.5	...	...	...
MnSi No. 12	4.6	900	8.6	3.2	...	...	...
MnSi No. 12	4.6	anneal at 1300 K	8.6	22.8	...	...	...
$Mn_{0.25}Si_{0.75}$ No. 1	7.1	370	270	0.17	...	...	...
$Mn_{0.35}Si_{0.65}$ No. 1	8.2	370	150	0.48	...	...	...
$Mn_{0.4}Si_{0.6}$ No. 1	5.6	370	36	0.68	0.80	0.23	0.033
$Mn_{0.6}Si_{0.4}$ No. 1	4.1	370	24	0.87	0.93	0.07	0.028
$Mn_{0.65}Si_{0.35}$ No. 1	23.7	370	31	...	...	...	...
$Mn_{0.75}Si_{0.25}$ No. 1	6.3	370	7.7	1.09	...	...	...

8 and Table II). The negative TCR of amorphous films can be fitted by two different functional forms. In Fig. 6 the data were fitted to the empirical relation

$$\rho(T)/\rho(4.2\ \mathrm{K}) = A + Be^{-CT}, \qquad (1)$$

where the values of the constants A, B, and C are listed in Table II. The functional form (1) was first suggested by Gudmundsson *et al.*[17] for the amorphous magnetic system $(Fe_{1-x}Mn_x)_{75}P_{16}B_6Al_3$ with $0.1 \leq x \leq 1.0$. A few remarks are pertinent to such a fit. First, the fit only works for compositions close to MnSi where the ratio $\rho(T)/\rho(4.2\ \mathrm{K})$ is fairly close to unity. Second, as seen in Fig. 6 the fit works fairly well except for a few irreversible jumps in the resistivity which result from microcracks at the contacts caused by the extreme brittleness of the material. Third, the fact that such a smooth fit of the data is possible suggests

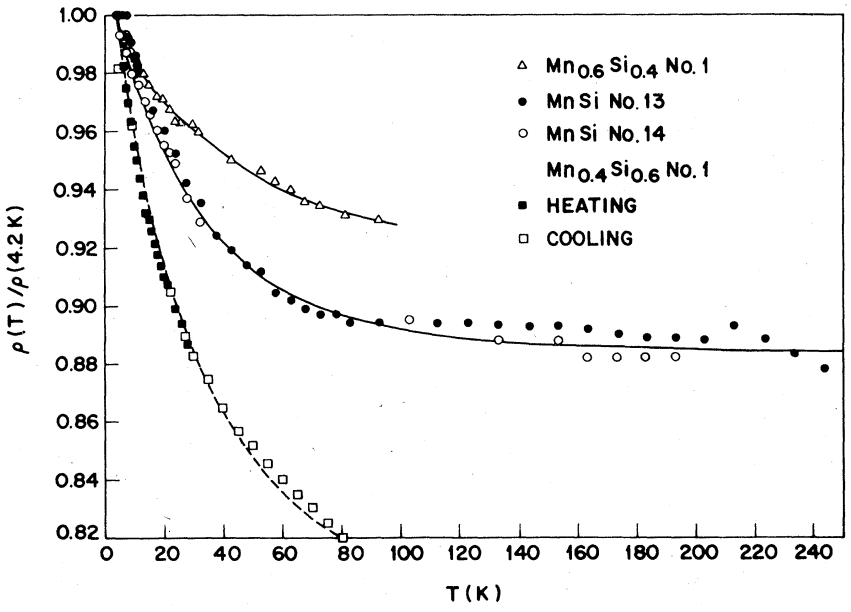

FIG. 6. Temperature dependence of the resistivity for a-Mn-Si films. The curves represent data fitting to the functional form $\rho(T)/\rho(4.2\ \mathrm{K}) = A + Be^{-CT}$ (values of the constants A, B, and C are listed in Table II).

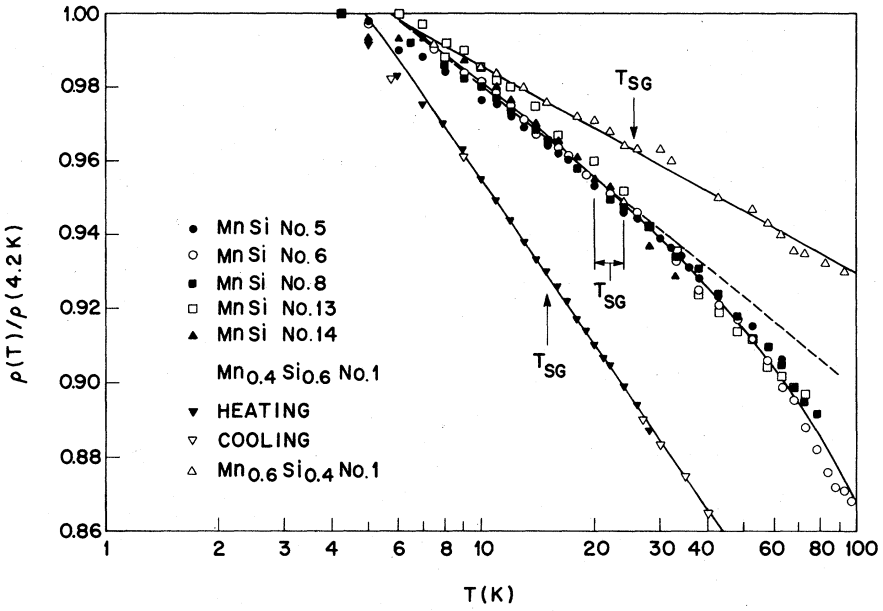

FIG. 7. Temperature dependence of the resistivity for a-Mn-Si films. The vertical bars around T_{SG} indicate the spread in T_{SG} as measured by susceptibility on a-MnSi films.

that the resistive data do not exhibit any anomaly in the vicinity of spin-glass transition temperature (T_{SG}) defined as the temperature corresponding to the susceptibility maximum. Finally, it is interesting to point out that the exponential constant C of relation (1) has values (Table II) in very good agreement with the values obtained in $(Fe_{1-x}Mn_x)_{75}P_{16}B_6Al_3$ for $x > 0.5$. On the other hand, the resistivity can be plotted versus $\log T$ (Fig. 7), which is more usual for magnetic systems. It can be seen from Fig. 7 that the smooth line fit of the data for a-MnSi films deviates from the straight line fit (dashed line) in the vicinity of T_{SG}. One should, however, be careful in identifying this resistive behavior with T_{SG} because as shown in Fig. 7 the same is not possible for off-stoichiometric films; the resistivities of $Mn_{0.4}Si_{0.6}$ and $Mn_{0.6}Si_{0.4}$ do not show any pronounced deviation from the straight line fit at their respective T_{SG}.

The smoothness of the resistivity in the vicinity of T_{SG} is not surprising. Indeed, it has been shown

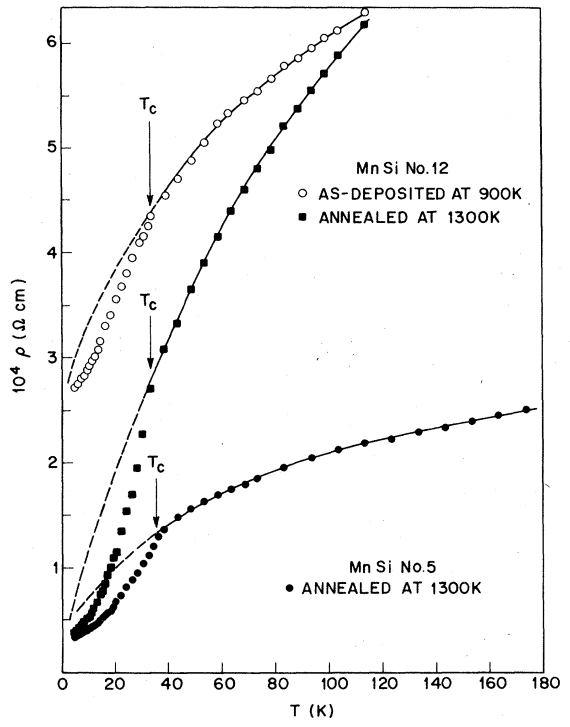

FIG. 8. Temperature dependence of the resistivity for crystalline MnSi films displaying the Curie temperature (T_C) anomaly.

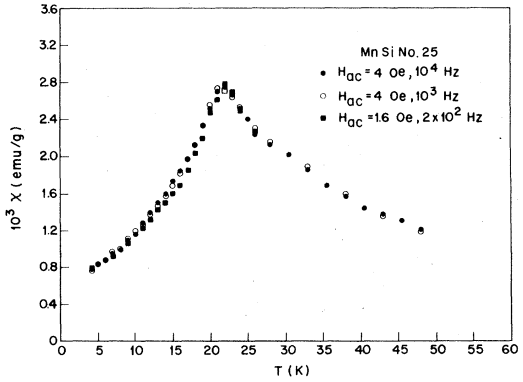

FIG. 9. Susceptibility vs temperature showing the independence of the measurement on frequency.

theoretically[18-20] that in the vicinity of magnetic critical points, $d\rho(T)/dT$ varies as the magnetic specific heat. Since the magnetic specific heat (see Sec. D and Fig. 18) only displays a very small anomaly near T_{SG}, one would at most expect a small anomaly in $d\rho(T)/dT$ which is consistent with a smooth variation of $\rho(T)$ near T_{SG}.

The metallic behavior (positive TCR) of crystalline films is clearly demonstrated in Fig. 8. It is also clear from Fig. 8 that the resistivity of recrystallized a-MnSi No. 5 (see Fig. 7 for its resistivity in the amorphous state) is quite similar to that of an as-deposited crystalline film (MnSi No. 12). The room-temperature resistivity of MnSi No. 5 is close to that reported for bulk[16]; the higher room-temperature resistivity of MnSi No. 12 is caused by the large surface area of the film resulting from the platelet morphology of the as-deposited crystalline film (Fig. 4). The high purity of the films is demonstrated by the resistivity ratio $\rho(RT)/\rho(4.2\text{ K})$ of 23 measured on annealed MnSi No. 12 as compared to 50 for a zone-refined single crystal.[16] In further agreement with bulk,[16] one also observes a sharp change in TCR near $T_C \simeq 30$ K (Fig. 8).

The different sign of the TCR for amorphous and crystalline films is also useful to study films deposited in the transition region ($T_D = 650$ K). It was concluded from the structural analysis of MnSi Nos. 15 and 20 (Sec. III A) that these films consisted of isolated 1-μm microcrystals embedded in an amorphous matrix. This conclusion is supported by the resistive data shown in Table II; these films have a negative TCR because the current is carried by the amorphous matrix.

In conclusion, although the measurement of the resistivity does not provide an unambiguous determination of T_{SG}, its temperature dependence clearly separates amorphous from crystalline films.

C. Susceptibility measurements

The main features of the susceptibility measurements, i.e., the cusp and its dependence on T_D as well as the anomaly near $T_C \simeq 30$ K have been previously discussed.[8] The cusp and the anomaly at 30 K (revealed by a downward rather than upward concavity in the susceptibility curve) are shown again in Fig. 9. It is also clear from Fig. 9 that the spin-glass susceptibility peak is independent of frequency at least down to 200 Hz. Since, as we shall see later the dc susceptibility below T_{SG} is different from the ac susceptibility, this implies that the pertinent relaxation times are between 5 $\times 10^{-3}$ sec and several seconds. Because of the anomaly at 30 K and the increasing χ and R with T_D (Table III and Table I of Ref. 8), it was concluded that amorphous MnSi contains clusters of Mn atoms. It was assumed that the intracluster interaction was ferromagnetic[8] because the susceptibility anomaly occurs very close to the ferromagnetic T_C of 30 K of crystalline MnSi. This assumption will be confirmed later on by the high-temperature dc susceptibility measurement. It was further assumed that these clusters were amorphous. Al-

TABLE III. Properties of the Mn-Si susceptibility samples.

Sample No.	Thickness (μm)	T_D (K)	$10^3\chi$(4.2 K) (emu/g)	$p_{eff}(\mu_B)$	T_{SG} (K)	R[a]
MnSi No. 11[b]	7.3	77	0.20	2.7	24	2.2
MnSi No. 11[b]	7.3	anneal at 300 K	0.44	3.4	20	2.2
MnSi No. 28	62.4	350	0.62	5.2	22	3.3
MnSi No. 26[b]	8.6	370	0.77	5.4	23	3.2
MnSi No. 25[b]	11.4	370	0.77	6.2	22	3.6
MnSi No. 27[b]	33.6	370	0.84	6.7	22	3.7
MnSi No. 21[b]	4.4	525	0.70	6.3	21	4.0
MnSi No. 22[b]	5.9	625	1.01	6.7	23	4.3
MnSi No. 23[b]	4.4	675	2.03	...	24	1.8
MnSi No. 23[b]	4.4	anneal at 1300 K	4.25	...	...	...
$Mn_{0.35}Si_{0.65}$ No. 1	6.3	370	0.53	2.1	6.5	1.3
$Mn_{0.4}Si_{0.6}$ No. 1	4.2	370	0.62	...	15	2.1
$Mn_{0.4}Si_{0.6}$ No. 2	12.1	370	0.64	3.7	13	2.0
$Mn_{0.6}Si_{0.4}$ No. 1	3.7	370	0.52	4.9	25.5	2.9
$Mn_{0.6}Si_{0.4}$ No. 2	17.0	370	0.34	3.7	26	2.8
$Mn_{0.65}Si_{0.35}$ No. 1	21.4	370	0.14	2.0	23.5	2.2
$Mn_{0.7}Si_{0.3}$ No. 1	57.6	370	0.10	1.9	22	2.0

[a] $R = \chi(T_{SG})/\chi(4.2\text{ K})$.

[b] These samples were already discussed in Ref. 8.

though it is hard (if not impossible) to rule our microscopically small crystalline clusters, this hypothesis is highly unlikely for the following reasons. First, as shown by the structural study (Sec. III A) the first appearance of crystallinity (as detected by x-ray diffraction and SEM) occurs at 650 K. Furthermore, when films such as Nos. 15, 20, and 24 contain crystalline islands (see Table I and Fig. 5 and Table I in Ref. 8), the susceptibility ratio $R = \chi(T_{SG})/\chi(4.2\ \mathrm{K})$ starts to decrease (Table I in Ref. 8). This decrease in R is shown in Fig. 10 for a microcrystalline film deposited at a temperature just above the threshold for crystallinity. Such a film is still microcrystalline as shown by the 70% increase in x-ray line intensity and by a tenfold decrease in the low-temperature resistivity resulting from the 1300-K anneal. As shown in Fig. 10 this annealing treatment completely eliminates the spin-glass transition and results in a temperature-independent susceptibility below $T_c = 30$ K in excellent agreement with bulk values.[16,21] Since crystallinity leads to a decrease in R, it is more than likely that the increase in R with T_D observed below 650 K is due to amorphous clusters.

At any rate, regardless of the exact structure of these clusters, the interaction between these clusters is still mediated by the same spin-glass exchange interaction which controls individual spins. This is supported by the fact that although χ, R, and the effective number of Bohr magnetons per Mn atom (p_{eff}) all increase with T_D (Table III and Table I or Ref. 8), T_{SG} remains fixed at 22 ± 2 K. Furthermore, the spin freezing which is thought to occur below T_{SG} and is measured by the spin-glass order parameter[6,8,22] $q(T)$ can be seen to be quite similar (Fig. 11 and Fig. 4 of Ref. 8) for films deposited at various T_D. The data shown in Fig. 11 are close to the predictions of mean-field theo-

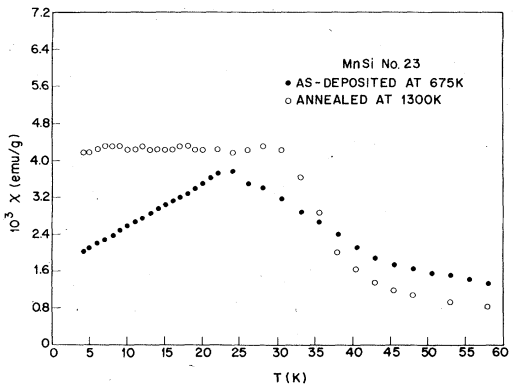

FIG. 10. Susceptibility vs temperature for a microcrystalline (as-deposited film) and a fully crystalline film (annealed at 1300 K).

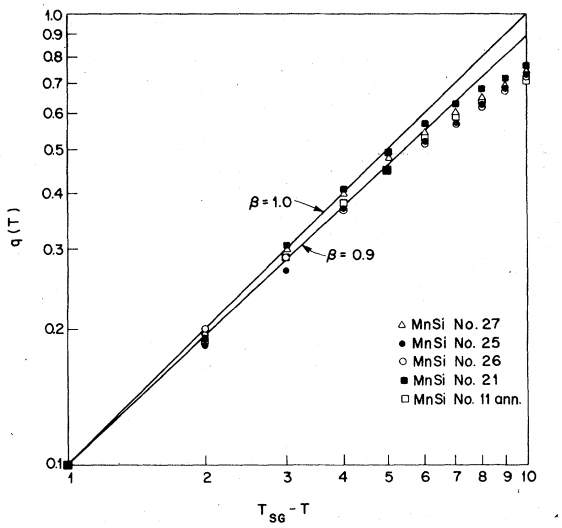

FIG. 11. Log-log plot of the order parameter $q(T)$ as a function of T_{SG}-T for various a-MnSi films.

ry, since a power law $q(T) \alpha (T_{SG} - T)^{\beta}$ with $0.9 \leq \beta \leq 1.0$ fits the data down to $T_{SG} - T = 5$ K. Similar results have been reported[6] for the concentrated spin glass a-$GdAl_2$. These experimental results will now be examined in the light of the cluster mean-field theory (CMFT) which suggests that the mean-field theory applicable to individual spins can be extended to a concentrated spin glass containing ferromagnetic clusters.[23-25]

Fitst of all, the existence of a cusp as T_D varies from 77 to 625 K (Fig. 3 of Ref. 8) is consistent with the prediction made by the CMFT that $\chi(T)$ always has a cusp at T_{SG} even in the presence of large ferromagnetic clusters[25] ($N \geq 12$, where N is the number of spins in a cluster). Furthermore, the deviations from mean-field theory shown by $q(T)$ (Fig. 4 of Ref. 8) are consistent with the CMFT in the sense that deviations from mean field are greater for the ferromagnetic than for the antiferromagnetic clusters and are quite pronounced for the ferromagnetic clusters with $N = 6$ (Fig. 3 of Ref. 24), which is a reasonable size to assume for the clusters of the present study. On the other hand, there is a marked disagreement between experiment and Eq. (7) of the CMFT[25] which can be rewritten

$$kT_{SG} = \bar{J} M_c , \tag{1}$$

where $\bar{J}$ is the near-neighbor intercluster exchange interaction and M_c is the value of the cluster moment at T_{SG}. Since the increase of χ and p_{eff} with T_D was linked with increased clustering, one would expect T_{SG} to increase with T_D in contradiction with experimental data ($T_{SG} = 22 \pm 2$ K). The in-

crease of χ and p_{eff} with T_D was related[8] to an increase in number *and/or* size of the Mn clusters. If the increase in p_{eff} by a factor of 2.5 (Table III) with T_D is due to an increase in the size of the clusters, then M_c and therefore T_{SG} should increase by 2.5 which is in marked disagreement with the invariance of T_{SG}. It is also possible that p_{eff} increases as a result of an increased number of clusters of approximately constant size. In this case no comparison can be made with the CMFT since there is no explicit dependence of T_{SG} on the number of clusters in the CMFT; indeed, $\bar{J}$ is an intensive variable just as the exchange interaction $\tilde{J}$ in the mean-field theory of individual spins.[26] Since the number and size of clusters is not known, one cannot conclude that relation (1) necessarily conflicts with experiment. Furthermore, neither the CMFT nor the mean-field theory of individual spins represents a complete description of a-MnSi films which are undoubtedly composed of individual spins and clusters,[8] the latter increasing with T_D. Since the increased clustering with increasing T_D occurs at the expense of individual spins, and although the exchange field caused by a cluster may be larger by a factor M_c than the exchange field caused by an individual spin, this effect could be compensated by the fact that the clusters are much further apart than the individual spins.

One should also add that since χ, R, and p_{eff} increase with T_D as a result of these clusters, the smallest value of these parameters corresponds to the most random film deposited at 77 K (Table III). Although this film deposited at 77 K may not be completely random, the value for p_{eff} of 2.7 μ_B is within experimental error of the value reported[16] for a single Mn atom in crystalline MnSi (2.19 μ_B). This result would support the speculation that the spin-glass interaction (susceptibility peak) would still be present in a truly random alloy.

The purity of the a-MnSi films, which was already demonstrated by the x-ray diffraction and electrical properties of recrystallized films, can be further established by their magnetic properties. The magnetic properties of MnSi No. 25 in the amorphous *as*-deposited state and in the recrystallized state following a 1300 K anneal are shown, respectively, in Figs. 9 and 12. Both the saturation magnetization of 26.4± 1.3 emu/g and the T_C of 30 K are in excellent agreement with bulk properties.[16]

It has been suggested that the susceptibility cusps observed in spin glasses are artifacts of the ac technique.[27] However, Mizoguchi *et al.*[6] have shown "that such cusps are not artifacts of the measurement technique" by reporting a low-field dc susceptibility cusp on the concentrated $GdAl_2$ spin glass. A similar result has been recently observed

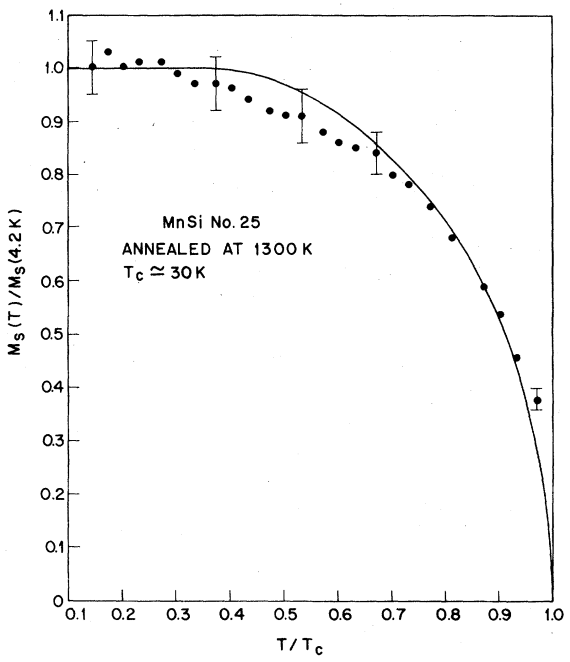

FIG. 12. Reduced saturation magnetization as a function of reduced temperature for a recrystallized MnSi film. The value of $M_S(4.2\ K)$ is 26.4 ± 1.3 emu/g as compared to 27 (Ref. 16). The solid line is the Brillouin function for $S=\frac{1}{2}$.

on the dilute Cu-Mn spin glass,[28] but only on samples cooled in zero field (a cooling field as small as 2 Oe was sufficient to eliminate the nearly symmetrical cusp). In order to establish whether a phase transition occurs at T_{SG}, it is important to know the frequency dependence of T_{SG}. The experimental results are divided on this question. On the one hand, Löhneysen *et al.*[29] report that T_{SG} decreases with decreasing frequency (0.02–1142 Hz) in $(La_{1-x}Gd_x)Al_2$. On the other hand, Hardiman[30] reports a frequency-independent (16 Hz–2.8 MHz) T_{SG} for dilute Ag-Mn spin glasses and attributes the frequency dependence observed in $(La_{1-x}Gd_x)Al_2$ to peculiarities of the Gd magnetism. The dc measurements shown in Fig. 13, although not obtained with as low a magnetic field, support the idea that the spin-glass transition is not an artifact of the ac technique. Indeed, although the ac and dc susceptibilities differ below $T_{SG\,dc}$ (defined as the temperature corresponding to the maximum dc susceptibility), they are in agreement within experimental error above $T_{SG\,dc}$. Furthermore, $T_{SG\,dc}$ is in very good agreement with the temperature at which the ac susceptibility starts to decrease. This result, taken in conjunction with the independence of T_{SG} on frequency in the range $200–10^4$ Hz (Fig. 9), would tend to agree with the results on Ag-Mn.[30] Consequently, the basic dif-

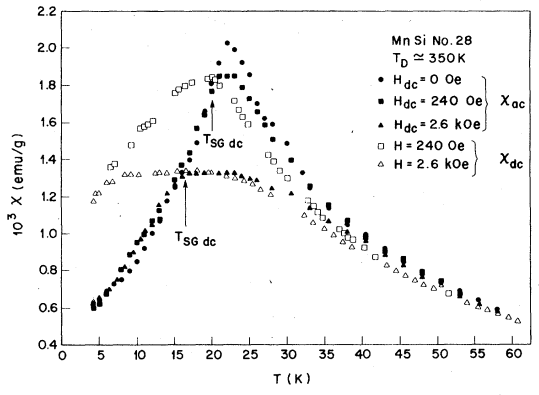

FIG. 13. Susceptibility measurements (ac and dc) as a function of temperature. The arrows indicate the maximum susceptibility of the dc measurement.

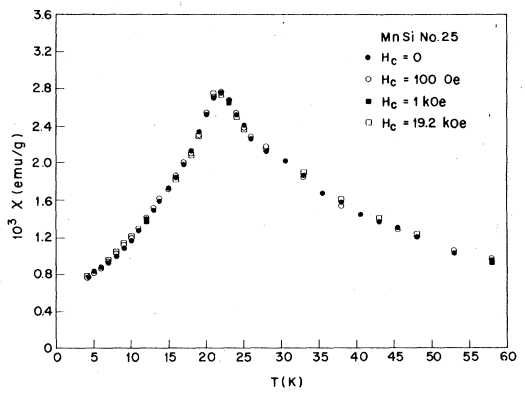

FIG. 15. Temperature dependence of the susceptibility measured in zero applied dc field (H_{ac} = 4 Oe) after cooling from 70 to 4.2 K in various applied dc fields (H_c).

ference between ac and dc susceptibility measurements on a spin-glass resides in the fact that the dc susceptibility decreases less rapidly with decreasing temperature below T_{SG}. On the other hand, at low temperatures the dc susceptibilities measured in different magnetic fields become equal in a similar way to the ac susceptibilities. The slope of the inverse dc susceptibility decreases steadily with decreasing temperature and the value of p_{eff} obtained from the various slopes (Fig. 14) is always larger, (2.6–4.8) μ_B, than the value reported[16] in crystalline MnSi for a single Mn atom (2.19 μ_B). Both these observations are consistent with the presence of ferromagnetic clusters previously postulated on the basis of the 30-K anomaly and the dependence of χ on T_D. The low-temperature value of p_{eff} (4.8 μ_B) obtained from the dc measurement (Fig. 14) is in good agreement with the corresponding ac measurement (Table III).

It is well known that the magnetic properties of spin-glasses are altered when the samples are cooled in a magnetic field. Although the susceptibility peak remains unchanged after cooling in magnetic fields as high as 19.2 kOe (Fig. 15), this field cooling results in a displaced hysteresis loop as a result of the frozen-in moment. The ferromagnetic clusters can be evidenced directly by the hysteresis loop shown in Fig. 16. If one takes the ratio of the saturation magnetization of Fig. 16 (2 emu/g) to that measured on bulk MnSi (27 emu/g), one concludes that the ferromagnetic clusters represent approximately 7% of the sample.

Further information about the spin-glass transition can be obtained by studying the magnetic field dependence of the susceptibility cusp. This effect was already briefly discussed in Fig. 2 of Ref. 8 and in Fig. 13 of the present study. However, the data are best analyzed by plotting the field susceptibility χ_H [$\chi_H = \chi(T_{SG}, 0) - \chi(T_{SG}, H)$] as a function

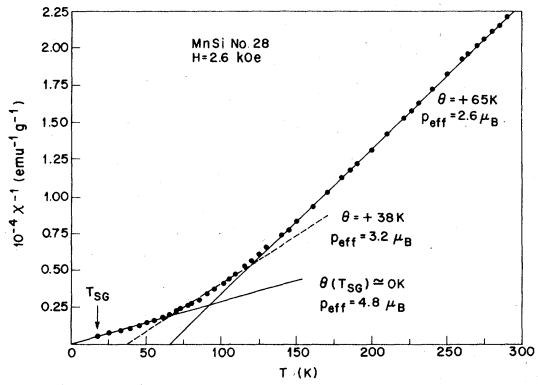

FIG. 14. Temperature dependence of the inverse dc susceptibility obtained in a 2.6-kOe applied field showing various Curie-Weiss behaviors.

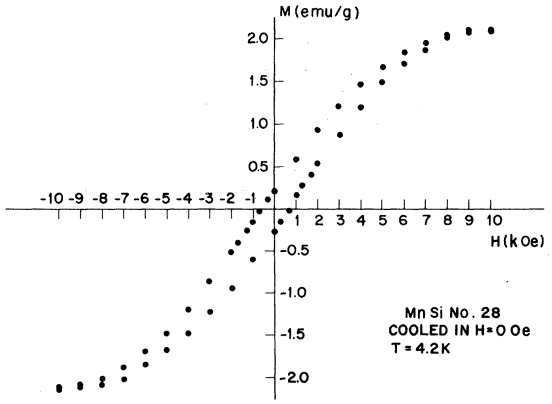

FIG. 16. Hysteresis loop showing small remanence ($\simeq$ 2 emu/g).

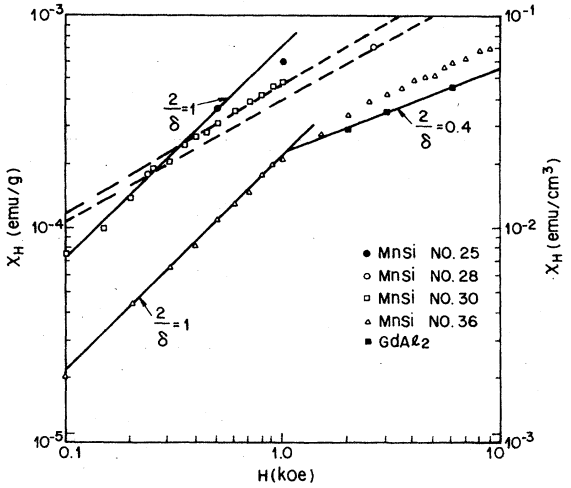

FIG. 17. Field susceptibility χ_H at T_{SG} as a function of magnetic field for various MnSi films (left-hand ordinate axis) and for the $GdAl_2$ data of Ref. 6 (right-hand ordinate axis).

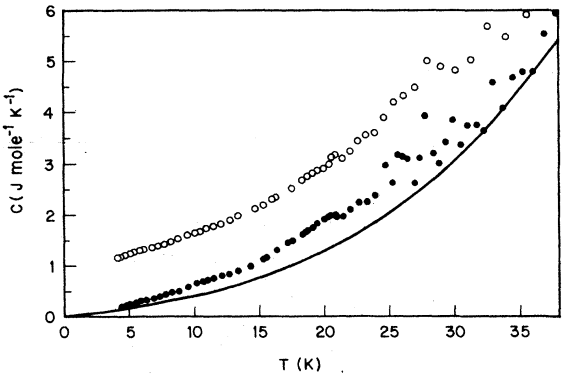

FIG. 18. Specific heat of a-MnSi no. 28 (solid points) and a-MnSi No. 35 (open dots) as a function of temperature. The solid line represents the electronic and lattice specific heat calculated as shown in the text. The data for a-MnSi No. 35 have been displaced upward by 1 J mole^{-1} K^{-1} for clarity.

of magnetic field as shown in Fig. 17 for both the partial previous data and more-detailed additional data. The interest of such a plot stems from the fact that the critical exponent δ can be extracted from χ_H. Indeed, Chalupa[31] has pointed out that

$$q(T_{SG}) \sim \chi_H(T_{SG}, H) \sim H^{2/\delta} \tag{2}$$

Consequently, a plot of log$q$ or logχ_H vs log H yields a slope $2/\delta$. The Monte Carlo studies of an Ising spin glass in terms of clusters[32] resulted in a log-log plot of q vs H with a slope of 0.41 or $\delta = 4.9$. This value is in very good agreement with the value obtained by Chalupa[31] in his analysis of the $GdAl_2$ data[6] which are shown again in Fig. 17. There are two interesting points about the data shown in Fig. 17. First at high field, the slopes for MnSi vary between 0.61 and 0.49 corresponding to $3.3 < \delta < 4.1$ which is close to the value obtained with $GdAl_2$. Second, there is a definite crossover at low field to a value $\delta = 2$ (the mean-field value). One may speculate[33] that this crossover results from the fact that close to the critical T_{SG} the coupling between clusters is important, which is a long-range low-energy interaction, and mean-field theory applies, while far from T_{SG}, one gets a high-energy intracluster interaction and $\delta = 3-5$.

D. Specific-heat measurement

In contradistinction with the sharp cusp in χ at T_{SG}, the specific heat of spin-glasses shows either nothing[34] or a broad maximum[7] near T_{SG}. The specific-heat data shown in Fig. 18 were obtained from 4.2 K up to 40 K by smoothly increasing small increments of heat. The increments of heat varied from 3×10^{-4} to 3×10^{-2} J between 4.2 and 22 K and up to 3×10^{-1} J at 40 K. The points were taken approximately 0.5 K apart in times varying between 1.5 to 3 min. The specific heat of the sample was calculated by subtracting from the total specific heat the specific heat of a blank run containing the same amount of grease. The blank run with the apiezon grease yielded a structureless perfectly smooth curve and consequently any structure in the specific-heat data of Fig. 18 is an intrinsic property of the sample. It is quite clear from Fig. 18 that a small maximum is present in the vicinity of $T_{SG} \simeq 21$ K. This small maximum is reproducible first as a function of runs (three different runs on both samples yielded essentially the same curve) and for two different samples. As a matter of fact, although the run with MnSi No. 35 contained 20% more MnSi and 30% less grease, both the maximum and even the absolute value of the specific heat (within a few %) are reproducible, as can be seen from Fig. 18. In order to obtain the magnetic heat capacity it is necessary to subtract the electronic and lattice contributions. This presents some difficulties since it is hard to estimate these parameters even in the crystalline state.[35,36] By subtracting on a C/T vs T^2 plot a line tangential to the specific-heat curve above and below $T_C = 30$ K, Fawcett *et al.*[35] obtained an electronic term $\gamma_e = 3.55\times10^{-2}$ J mole^{-1} K^{-2} and a Debye temperature $\Theta_D = 453$ K. The same procedure was used to obtain the solid curve shown in Fig. 18; the crystalline value of γ_e was used for the amorphous data and the lattice contribution was obtained by letting the lowest specific-heat data points obtained above T_{SG} lie above or on the solid curve. Such a fit re-

sulted in $\Theta_D = 296$ K for a-MnSi. The ratio of Θ_D (amorphous) to Θ_D (crystalline) is 0.65, which is very close to the value of 0.64 reported[7] for $GdAl_2$. Subtracting the solid curve of Fig. 18 from the data points yields the magnetic specific heat C_m which exhibits a small maximum near 20 K. C_m varies approximately as $T^{3/2}$ below 20 K, which is similar to the temperature dependence of C_m reported[7] for a-$GdAl_2$. The magnetic entropy at 21 K is 0.75 $J\,mole^{-1}K^{-1}$, which is only 0.13 of $R\ln(2S+1)$ for $S=\frac{1}{2}$. This result suggests two remarks. First, even the entropy associated with magnetic ordering in the crystalline state is very small[36] (0.38 $J\,mole^{-1}K^{-1}$). Second, the entropy associated with a spin-glass transition is small in general: 0.55 $R\ln(2S+1)$ for a-$GdAl_2$,[7] 0.22 $cR\ln(2J+1)$ for $Au_{0.92}Fe_{0.08}$,[37] and 0.33 $cR\ln(2J+1)$ for Cu-Mn alloys[34] (c being the concentration of Fe or Mn).

The significance of the small specific bump will now be discussed in the light of existing theories. The apparent contradiction in the mean-field theory between the presence of a sharp cusp in the susceptibility and the smooth behavior of the specific heat has been explained by Anderson[38] in terms of clusters. These clusters have a temperature-dependent size and consist of correlated spins within a correlation length $\xi(T)$ which increases to ∞ at T_{SG}. These clusters must not be mistaken with the clusters of the present study or of the CMFT[24] which arise from statistical or chemical clustering. These temperature-dependent clusters can explain the strong magnetic field dependence of the susceptibility cusp which is displayed in Fig. 17. If one uses the scaling law $\alpha = 2 - \beta(1+\delta)$, where $-\alpha$ is the specific-heat critical exponent, Chalupa[31] and Anderson[38] have argued that a value of $\delta \simeq 5$ implies $\alpha = -3$ which is consistent with the smooth appearance of the specific heat near T_{SG}. The crossover to $\delta = 2$ (mean-field value) at low fields coupled with the somewhat lower values of δ at high fields as compared to $GdAl_2$ would imply $\alpha = -1$ to -2, which would be consistent with a small bump at T_{SG}. Furthermore, the CMFT is also in agreement with the specific-heat bump at T_{SG} since this theory has established that while the specific-heat cusp predicted by the mean-field theory becomes rapidly eliminated in the presence of antiferromagnetic clusters,[24] it remains even in the presence of concentrated ferromagnetic clusters.[25]

Finally, one observes in Fig. 18 a striking dispersion of data points above $T_{SG} \simeq 21$ K. It is important to understand that this is not scatter; each data point was obtained sequentially with increasing temperature. Although the points cannot be reproduced from run to run, each run results in a similar dispersion of points above T_{SG}. Furthermore, this dispersion is definitely an intrinsic property of a-MnSi since, as mentioned above, an identical blank run with the same amount of grease yields a monotonically smooth increasing specific heat. One should also point out that this dispersion is only observed in the specific-heat experiments and not in the susceptibility or resistivity measurements. It may also be noteworthy that the dispersion in the specific-heat data occurs approximately over the same range of temperature as the susceptibility anomaly. Furthermore, similar dispersions have been seen (although not discussed) in other spin-glasses. For example, a pronounced dispersion can be seen[7] for a-$GdAl_2$ and a weaker one for Cu-Mn alloys (see in particular Fig. 3 of Ref. 34). Although the cause for this dispersion is not understood, we would like to speculate that it is caused by the magnetic ordering taking place at various temperatures in clusters of different sizes.

E. Off-stoichiometric a-Mn-Si alloys

The electrical properties of off-stoichiometric a-Mn-Si were already briefly discussed in conjunction with the electrical properties of a-MnSi. It is clear from Figs. 6 and 7 and from Table II that the electrical properties of off-stoichiometric films are quite similar to those of stoichiometric a-MnSi films; a-Mn-Si films have a negative TCR. Furthermore, $\rho(RT)/\rho(4.2\text{ K})$ decreases while $\rho(RT)$ increases with increasing Si content (Table II). This is consistent with the fact that as one increases the number of covalent Si bonds, one approaches a regime of hopping conductivity characteristic of a-Si doped with Mn.[39] On the other hand, Mn-rich films eventually (75 at.% Mn) become similar to Mn and display a positive TCR.

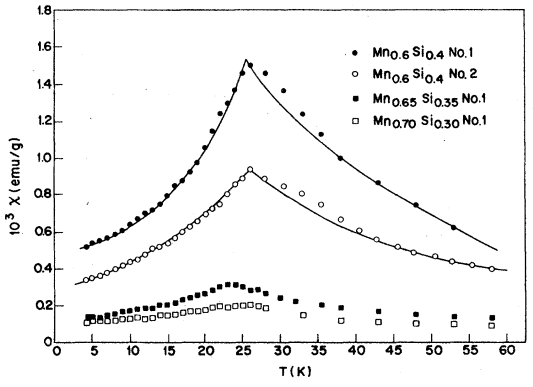

FIG. 19. Susceptibility vs temperature for a-Mn-Si films on the Mn-rich side of MnSi.

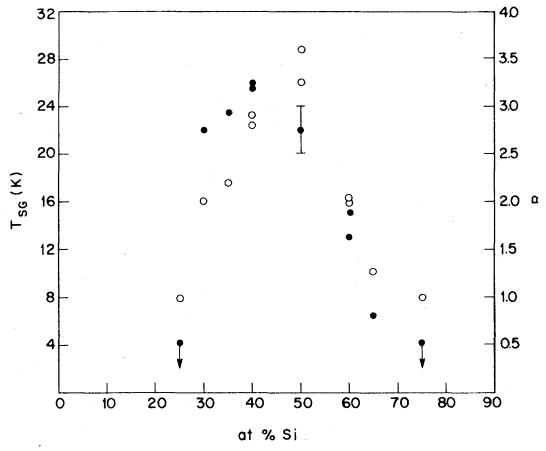

FIG. 20. Spin-glass temperature (T_{SG}) (closed circles) and susceptibility ratio $R = \chi(T_{SG})/\chi(4.2\ \mathrm{K})$ (open circles) for all a-Mn-Si alloy films.

The magnetic susceptibility of a-Mn-Si films is consistent with the electrical properties. The temperature dependence of the susceptibility for Mn-rich films is shown in Fig. 19. As one increases the Mn content starting from MnSi, T_{SG} increases to 26 K (Fig. 19 and Table III), while the ferromagnetic anomaly becomes more pronounced but remains centered around 30 K. This result is consistent with the well known fact that T_{SG} increases with the concentration of magnetic atoms. Furthermore, this result is also consistent with the model proposed for a-MnSi; indeed, one would expect the number and size of the ferromagnetic clusters to increases with increasing Mn content. On the other hand, if one further increases the Mn content, T_{SG} and χ decrease (Figs. 19 and 20 and Table III) as one would expect from the increasing amount of antiferromagnetic behavior suggested from the electrical measurements. The behavior of Si-rich films is also consistent with the increasing number of covalent Si bonds suggested from the electrical measurements; both T_{SG} and R decrease rapidly with increasing Si content (Fig. 20 and Table III).

IV. SUMMARY AND FUTURE WORK

The properties of a-MnSi films are consistent with a model of ferromagnetic Mn clusters (most probably amorphous) embedded in an amorphous MnSi matrix. These clusters are mediated by the same spin-glass exchange interaction which controls individual Mn spins and results in a spin-glass transition of 22 K. The properties of off-stoichiometric films are consistent with the model proposed for a-MnSi. The properties reported here for a-MnSi are characteristics of pure MnSi, since recrystallized films regain all the properties (x-ray structure, resistivity and resistivity ratio, magnetic susceptibility, and magnetization of zone-refined single crystalline MnSi.)

The dependence of T_{SG} on stoichiometry implies a dependence of T_{SG} on separation between Mn atoms. The fact that the magnetic properties of crystalline Mn alloys and compounds depend strongly on the distance between Mn atoms is a well known fact (e.g., Heusler alloys). In order to study the effect of Mn-Mn distance on T_{SG}, it is planned to study various Mn-X alloys, where X are atoms with a different diameter than Si.

ACKNOWLEDGMENTS

We would like to thank R. C. Sherwood for several illuminating discussions on crystalline MnSi and S. Kosinski for her very able technical assistance.

[1]V. Canella, J. A. Mydosh, and J. I. Budnick, J. Appl. Phys. 42, 1689 (1971).
[2]V. Canella and J. A. Mydosh, Phys. Rev. B 6, 4220 (1972).
[3]V. Canella, in *Amorphous Magnetism*, edited by H. O. Hooper and A. M. de Graff (Plenum, New York, 1973), p. 195.
[4]R. W. Tustison and P. A. Beck, Solid State Commun. 20, 841 (1977).
[5]M. B. Salamon and R. M. Herman, Phys. Rev. Lett. 41, 1506 (1978).
[6]T. Mizoguchi, T. R. McGuire, S. Kirkpatrick, and R. J. Gambino, Phys. Rev. Lett. 38, 89 (1977).
[7]J. M. D. Coey, S. Von Molnar, and R. J. Gambino, Solid State Commun. 24, 167 (1977).
[8]J. J. Hauser, Solid State Commun. 30, 201 (1979).
[9]J. J. Hauser, Phys. Rev. B 5, 110 (1972).
[10]R. W. Tustison, Solid State Commun. 19, 1075 (1976).
[11]P. A. Beck, Prog. Mater. Sci. 23, 1 (1978).
[12]J. J. Hauser and J. V. Waszczak, Phys. Rev. B 18, 6206 (1978).
[13]I am indebted to J. E. Bernardini for the preparation of the targets.
[14]J. J. Hauser and C. M. Antosh, Rev. Sci. Instrum. 47, 156 (1976).
[15]F. J. DiSalvo, B. G. Bagley, R. S. Hutton, and A. H. Clark, Solid State Commun. 19, 97 (1976).
[16]J. H. Wernick, G. K. Wertheim, and R. C. Sherwood, Mat. Res. Bull. 7, 1431 (1972).
[17]H. Gudmundsson, H. U. Aström, D. New, K. V. Rao, and H. S. Chen, J. Phys. (Paris) Colloq. Suppl. 39, C-6-943 (1978).
[18]M. E. Fisher and J. S. Langer, Phys. Rev. Lett. 20, 665 (1958).

[19]T. G. Richard and D. J. W. Geldart, Phys. Rev. Lett. 30, 290 (1973).
[20]T. G. Richard and D. J. W. Geldart, Phys. Rev. B 15, 1502 (1977).
[21]The low-field dc bulk susceptibility retains a constant value of 4.25×10^{-3} emu/g up to 30 K [R. C. Sherwood (private communication)].
[22]S. F. Edwards and P. W. Anderson, J. Phys. F 5, 965 (1975).
[23]C. M. Soukoulis and K. Levin, Phys. Rev. Lett. 39, 581 (1977).
[24]C. M. Soukoulis and K. Levin, Phys. Rev. B 18, 1439 (1978).
[25]C. M. Soukoulis, Phys. Rev. B 18, 3757 (1978).
[26]D. Sherrington and S. Kirkpatrick, Phys. Rev. Lett. 35, 1792 (1975).
[27]J. L. Tholence and R. Tournier, J. Phys. (Paris) Colloq. 35, C4-229 (1974).
[28]S. Nagata, P. H. Keesom, and H. R. Harrison, Phys. Rev. B 19, 1633 (1979).
[29]H. V. Löhneysen, J. L. Tholence, and R. Tournier, J. Phys. (Paris) Colloq. 39, C6-992 (1978).
[30]M. Hardiman, Bull. Am. Phys. Soc. 24, 262 (1979).
[31]J. Chalupa, Solid State Commun. 24, 429 (1977).
[32]D. Stauffer and K. Binder, Z. Phys. B 30, 313 (1978).
[33]J. Chalupa (private communication).
[34]L. E. Wenger and P. H. Keesom, Phys. Rev. B 13, 4053 (1976).
[35]E. Fawcett, J. P. Maita, and J. H. Wernick, Int. J. Magn. 1, 29 (1970).
[36]E. Fawcett (private communication); Ref. 13 of Y. Ishikawa, G. Shirane, and J. A. Tarvin, Phys. Rev. B 16, 4956 (1977).
[37]L. E. Wenger and P. H. Keesom, Phys. Rev. B 11, 3497 (1975).
[38]P. W. Anderson, J. Appl. Phys. 49, 1599 (1978); Lectures on Amorphous Systems, Summer School at Les Houches, France (1978) (unpublished).
[39]J. J. Hauser, Phys. Rev. B 9, 2544 (1974).

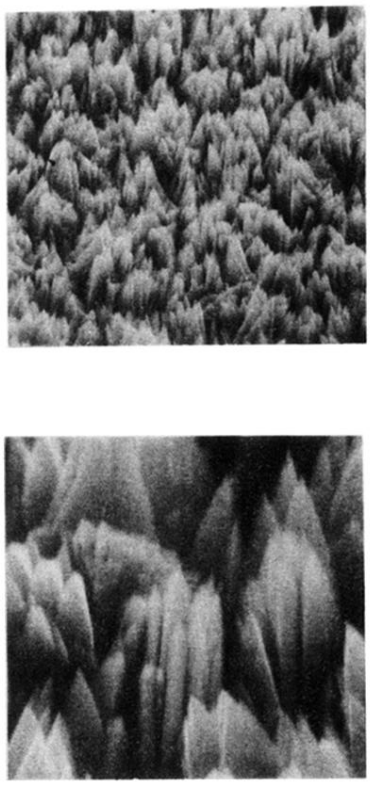

FIG. 4. Scanning electron microscopy for crystalline MnSi No. 12 deposited at 900 K (optical magnifications at 5000 $\tilde{\times}$ for the top picture and 20 000 $\tilde{\times}$ for the bottom).

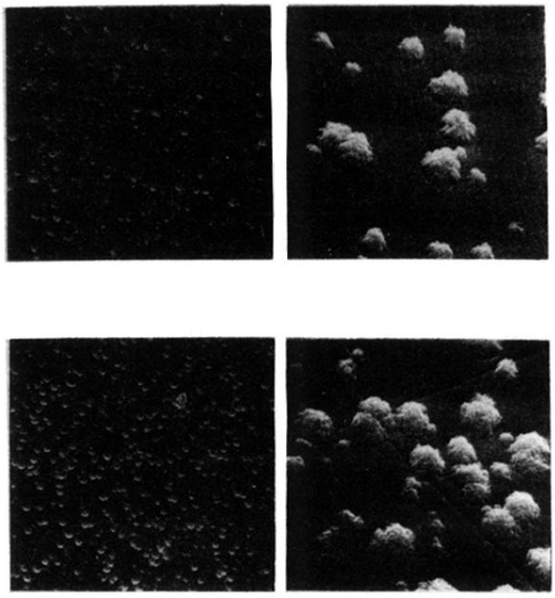

FIG. 5. Scanning electron microscopy for partially crystalline films deposted at 650 K: Top taken on MnSi No. 20 and bottom on MnSi No. 15 (the optical magnification are 1600× for the pictures on the left and 8000× for those on the right-hand side).